Letters

Discovery of Novel Myc−Max Heterodimer Disruptors with a Three-Dimensional Pharmacophore Model

Gabriela Mustata,*,† Ariele Viacava Follis,‡ Dalia I. Hammoudeh,‡ Steven J. Metallo,‡ Huabo Wang,§ Edward V. Prochownik,§ John S. Lazo,|| and Ivet Bahar†

Department of Computational Biology and Department of Pharmacology and Chemical Biology, University of Pittsburgh, Pittsburgh, Pennsylvania 15260, Department of Chemistry, Georgetown University, Washington, D.C. 20057, and Section of Hematology/Oncology Children's Hospital of Pittsburgh and The Department of Microbiology and Molecular Genetics, University of Pittsburgh Medical Center Rangos, Pittsburgh, Pennsylvania 15201

Received October 8, 2008

Abstract: A three-dimensional pharmacophore model was generated utilizing a set of known inhibitors of c-Myc−Max heterodimer formation. The model successfully identified a set of structurally diverse compounds with potential inhibitory activity against c-Myc. Nine compounds were tested in vitro, and four displayed affinities in the micromolar range and growth inhibitory activity against c-Myc-overexpressing cells. These studies demonstrate the applicability of pharmacophore modeling to the identification of novel and potentially more puissant inhibitors of the c-Myc oncoprotein.

Deregulation of the c-Myc oncogene is among the most frequent molecular abnormalities encountered in human cancer and is often associated with aggressive tumors of the breast, colon, cervix, lung, and hematopoietic organs.[1,2] c-Myc is a member of the basic helix−loop−helix leucine zipper protein family (bHLH-ZIP[a]) whose dimerization with another bHLH-ZIP protein, Max, is necessary for various biological activities, including cellular transformation, apoptosis, and transcriptional activation.[3–6] The fact that the oncogenic activity of c-Myc depends on its dimerization with Max makes the c-Myc−Max heterodimer not only an enticing target for drug design but also an important case study for the challenge of designing small molecule inhibitors of protein−protein interactions.[7,8]

Small molecules that specifically bind c-Myc and prevent c-Myc−Max heterodimerization have already been discovered.[9–13] Recent results from our group have provided NMR-based models showing that structurally unrelated inhibitors bind to distinct regions of the intrinsically unordered c-Myc monomer and alter its conformation to render it incapable of interacting with Max.[14]

Given the availability of the activity data for several c-Myc−Max heterodimer disruptors,[12,13] we decided to exploit this information to develop a molecule-derived pharmacophore model that would capture the primary chemical features common to these compounds. This is a powerful method for finding novel ligands and has been used extensively in drug discovery research in academia and the pharmaceutical industry.[15,16] Herein, we utilize GALAHAD (genetic algorithm with linear assignment for hypermolecular alignment of data sets),[17–19] implemented in SYBYL 8.0,[20] a recently developed pharmacophore modeling program that allows for full ligand flexibility while taking strain energy and steric overlap into account.

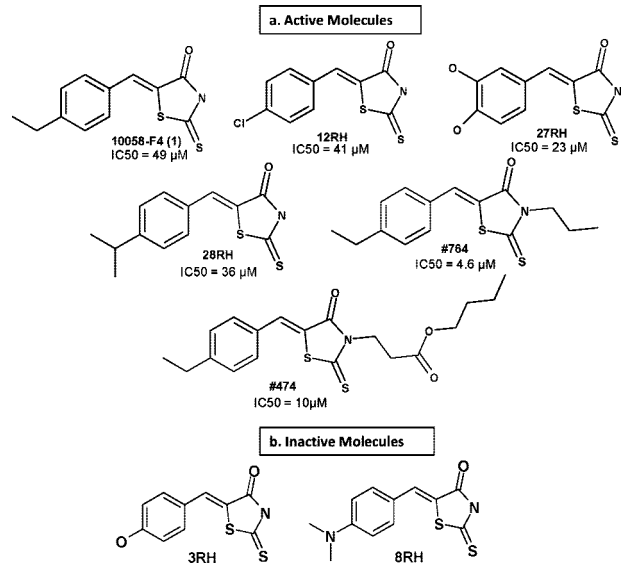

Figure 1. Molecules used in pharmacophore development: (a) active molecules used in the pharmacophore model generation with GALAHAD;[18] (b) inactive molecules used in the model refinement stage with TUPLETS.[20]

The data set used in these studies contains six c-Myc−Max heterodimer inhibitors identified previously by our group[12,13] (Figure 1a): the parental compound 10058-F4 (**1**)[13] and five of its derivatives.[12] All compounds bind to the same c-Myc region centered around residues Y402−K412,[14] with affinities that were up to 6- to 8-fold greater than that of **1**.[12,13] Twenty models were produced in our study, which differed somewhat in the number and type of features and in the conformations and overlay of the molecules. The pharmacophore model with the best overall score is displayed in Figure 2. It contains two hydrophobic features (yellow), one donor atom (blue), and two acceptor atoms (red).

The uniqueness of our approach is that the pharmacophore model generated by GALAHAD was further refined using two inactive analogues of **1** (Figure 1b). The refinement stage was performed using the Tuplets module in SYBYL 8.0,[20] which allows for the decomposition of the full pharmacophoric pattern found for each inactive ligand into its constituent distance multiplets, which are encoded into a vector fingerprint. Compounds retrieved in this way are often of a different chemical class than those used to generate the database query, demonstrating lead-hopping capability.

For validation purposes, the Tuplets refined model was used to query a test set of 10 compounds containing 6 active and 4

* To whom correspondence should be addressed. Phone: (412) 648-3333. Fax: (412) 648-3163. E-mail: gmustata@pitt.edu.
† Department of Computational Biology, University of Pittsburgh.
‡ Georgetown University.
§ University of Pittsburgh Medical Center Rangos.
|| Department of Pharmacology and Chemical Biology, University of Pittsburgh.

[a] Abbreviations: bHLH-ZIP, basic helix−loop−helix leucine zipper; GALAHAD, genetic algorithm with linear assignment for hypermolecular alignment of data sets; EMSA, electrophoretic mobility shifts assay.

10.1021/jm801278g CCC: $40.75
Published on Web 02/12/2009

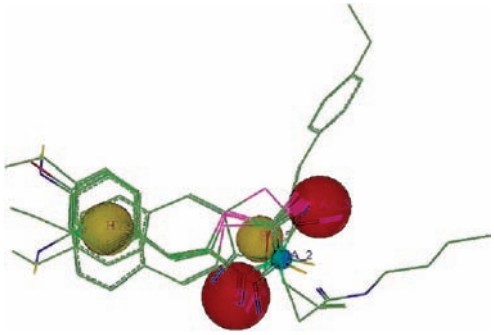

Figure 2. GALAHAD model obtained from six compounds in the biological data set includes two hydrophobes (yellow), one donor atom (blue), and two acceptor atoms (red). The sphere sizes indicate query tolerances.

inactive analogues of **1** (see Supporting Information) through a hierarchical clustering. The active compounds bind to the same c-Myc region centered around residues Y402−K412,[13] with affinities that were up to 6- to 8-fold greater than that of **1**.[11,12] All molecules performed acceptably well, with all actives compounds, except one, clustered together in the dendrogram, whereas the inactive ones were distributed. One of the inactive compounds was clustered together with the active compounds.

The resulting Tuplets hypothesis was further used to screen the ZINC 7.0 database[21] for druglike molecules (~5×10^6 compounds) that were sufficiently similar to the selected hypothesis. Note that the search database was translated into multiconformer Tuplets of the same type as the generated hypothesis. The hypothesis captured 15 822 hits (0.31% of database). The hits included a structurally diverse set of compounds as measured by their Tanimoto score of 0.5. This number progressively decreases with increasing Tanimoto similarity (e.g., 274 hits for 0.80 cutoff). Our choice of a Tanimoto cutoff of 0.5 is motivated by findings that similar biological activities may be shared by compounds that exhibit relatively weak structural similarities.[22–24] Although 2D similarity measures may overlook important structural/functional features and 3D metrics may retrieve compounds with more diverse topology, at the initial screening stage, 2D metrics are conveniently used for a rapid way of finding new lead compound. The top 100 compounds were filtered further for desirable ADME properties with ADME Boxes, version 4.0, software[25,26] to rationally deconvolute the large number of compounds that resulted from the initial database screening process, with the understanding that those compounds could potentially serve as drugs. The top-ranking 30 compounds were selected as potential candidates for the design of novel c-Myc inhibitors.

Given the extensive metabolism and rapid clearance of the parental **1**,[27] we selected for experimental testing those compounds that were predicted to be less metabolically labile. Considering that cytochrome P450 isoform CYP3A4 is the major enzyme responsible for xenobiotic metabolism in human organism and metabolizes >50% of drugs,[28] we used ToxBoxes, version 2.9,[29] to select compounds with the lowest predicted probability of being a CYP3A4 inhibitor at clinically relevant concentrations (K_i < 50 mM). Nine ZINC 7.0 compounds (Figure 3) were finally purchased from ChemBridge Corporation and tested in vitro for disruption of c-Myc−Max(S) heterodimer formation.

The experiments were performed as reported in our previous work[12] and are also available as Supporting Information. The compounds were screened in a circular dichroism assay where

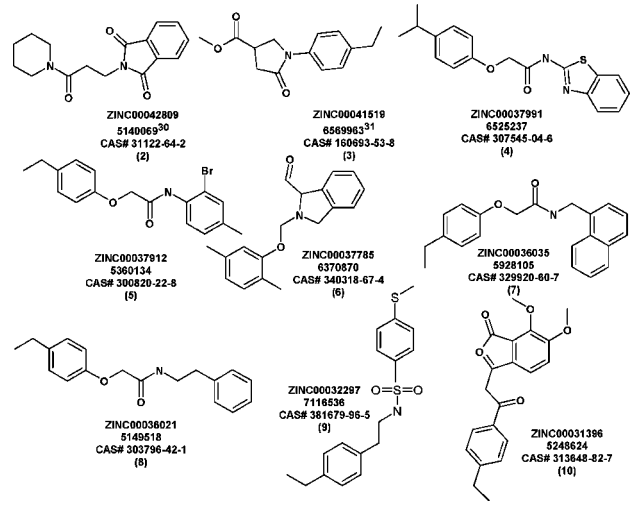

Figure 3. Compounds selected for experimental testing as potential c-Myc inhibitors (ZINC 7.0 and ChemBridge database numbering is indicated, as well as the CAS number).

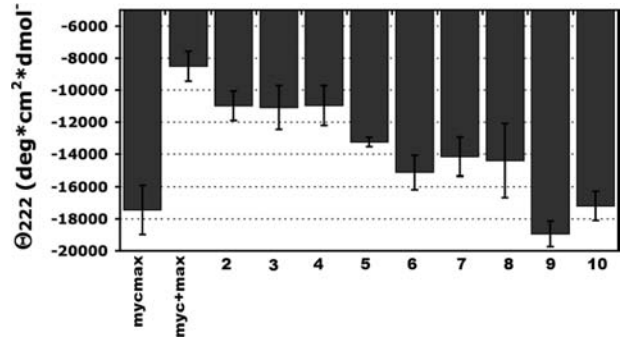

Figure 4. Disruption of 1.5 μM c-Myc−Max dimer by 200 μM concentration of each tested inhibitor measured by circular dichroism.[14] Data represent the average of three independent trials (error bars represent the standard error).

the helical content of equimolar mixtures of c-Myc and Max (1.5 μM) was determined from ellipticity measurements at 222 nm. Compounds capable of disrupting the protein dimer cause a decrease in helical content, as the isolated monomers are disordered and flexible. Initial screening of the nine compounds at one single high concentration (200 μM) indicated a nearly complete disruption of c-Myc−Max dimers being induced by four molecules, and partial disruption by another three (Figure 4). Only two compounds proved to be entirely inactive in this assay. These results support the reliability of the computational model in predicting active inhibitors.

The four compounds that exhibited the highest disruptive ability against c-Myc−Max(S) heterodimer formation at 200 μM were further tested over a range of concentrations, providing a full titration of the protein dimer disruption. Multiplication of the competition constant (K_{comp}), employed to fit the experimental data by the independently determined dissociation constant of c-Myc−Max dimers provided an estimate of the inhibitors affinity for c-Myc monomers (assuming that, like the set of compounds employed to generate the pharmacophore model, they interact exclusively with this protein monomer). The compounds displayed affinities in the mid-micromolar range, generally 2−10 times lower those of **1** and structurally related compounds employed to generate the pharmacophore model (Table 1).

The four compounds were tested further for direct competition to confirm that they interact directly with the c-Myc monomer

Table 1. Micromolar Affinities of the Best Tested Inhibitors for c-Myc As Estimated by Disruption of c-Myc−Max Dimers and Competition against the Parent Inhibitor **1** for Direct Binding to Monomeric c-Myc[a]

compd	c-Myc−Max disruption (μM)	competition against **1** (μM)
2[30]	10(3)	2.5(0.5)
3[31]	25(3)	40(10)
4	19(6)	18(6)
5	45(12)	70(20)

[a] Error ranges are indicated in parentheses. All the experiments were performed in triplicate.

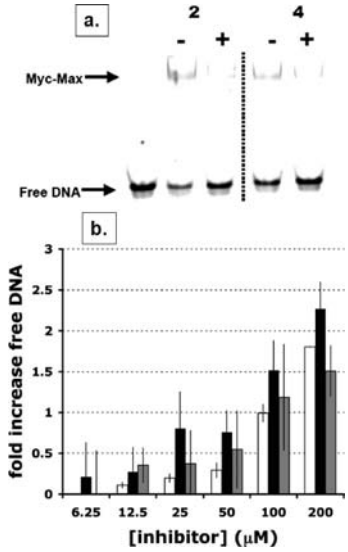

Figure 5. (a) Disruption of E-Box DNA binding by c-Myc−Max dimer by the two newly identified inhibitors with the highest binding affinity to c-Myc, **2** and **4**, at 200 μM. (b) Quantitative assessment of disruption of c-Myc−Max DNA binding for the parent **1** (white bars), **2** (black bars), and **4** (gray bars). Data represent the average of three independent trials (error bars represent standard error).

in a mode similar to that displayed by **1**. The compounds were tested by monitoring the fluorescence polarization of **1**, which is inversely proportional to the compound's tumbling rate in solution and increases when it is bound to the relatively large c-Myc (353−437) monomer. Under these conditions, all four compounds were able to displace **1** from c-Myc. A titration competition was performed for each compound, and data were fit in a similar way to the one described for the titrations of c-Myc−Max(S) disruption. K_{comp} in this case was multiplied by the dissociation constant of the complex between **1** and c-Myc to provide an estimate of the affinity of the tested compounds for c-Myc (353−437) binding. The obtained values were in reasonable agreement with the estimates of binding affinity obtained from the titrations of c-Myc−Max(S) dimer disruption. The two best compounds were also tested in an electrophoretic mobility shifts assay (EMSA) for disruption of DNA binding by c-Myc−Max(S) dimers, showing an inhibitory efficacy comparable to that of **1** (Figure 5).[12]

All nine compounds were tested in HL60 cells as described in our previous work[12] and also included as Supporting Information. As shown in Figure 6, compounds 5360134 (**5**) and 6370870 (**6**) proved to be significantly more active, with IC_{50} of 23 and 16.7 μmol, compared to 35 μmol for the parental **1**. The lack of exact correlation between the growth inhibitory effects of these compounds and their abilities to interact with c-Myc and disrupt c-Myc−Max association likely reflects the more complex nature of the cell-based assay, which requires uptake and retention of the compounds, their transport to the nucleus, and sufficient intracellular stability over the several

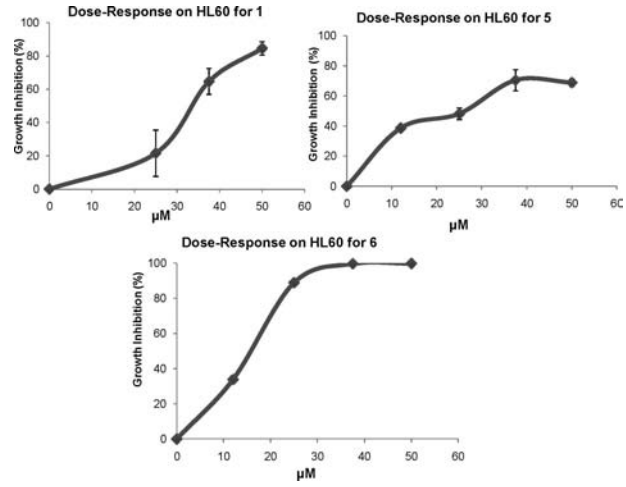

Figure 6. Dose−response profiles of **1**, **5**, and **6** on HL60 cell growth. IC_{50} values were calculated on the basis of dose−response profiles on day 5 following the addition of each compound.

day time span of the assay. Compounds **5** and **6** were tested with HL60 cells, with TGR1 (normal rat fibroblasts) along with TGR1 knockout cells with overexpressed HMGA1b (KO + HMG). These latter cells lacked c-Myc because of gene targeting; overexpression of the HMGAIb restored a normal growth rate in a c-Myc-independent manner.[32] Our results demonstrated very good inhibition in HL60 cells with both ZINC compounds and appeared to be somewhat selective in cells that expressed higher levels of c-Myc (HL60s) (see Supporting Information). They exerted the least effect on the KO + HMG cells and thus revealed a direct correlation between c-Myc levels and growth inhibition by these compounds. Further evidence for specificity came from the finding that **5** seemed to be more selective for HL60s than **6**. From these studies, we concluded that the ability of both ZINC compounds to inhibit the growth of mammalian cells is c-Myc dependent. These compounds were well within the range of what was seen when we screened a large number of **1** analogues.[12]

We recently identified the binding site and provided a model of the interaction between the parental **1**, and c-Myc.[14] The c-Myc−Max disruption assays and the competition assays clearly show that the active compounds described here bind in the same region as **1**, residues Y402−K412 of c-Myc. These compounds disrupt the formation of the highly ordered c-Myc−Max dimer by binding and stabilizing the intrinsically disordered monomer of c-Myc. NMR based studies of **1** binding to c-Myc demonstrated clear NOE signals with the binding site, but the overall flexibility of the disordered target resulted in insufficient NOE data to generate a standard structural model.[14] Disordered regions are overrepresented in disease related protein interactions; the ligand-based pharmacophore approach may be of especial importance in the search for inhibitors of these proteins.[33]

This is the first report of a pharmacophore model that provides a hypothetical picture of the main chemical features responsible for the activity of c-Myc−Max heterodimer disruptors that may prove to be useful for the future development of more potent analogues based on rational design. The newly identified lead compounds exhibit novel chemical scaffolds and will be further optimized to enhance their inhibitory activity.

Acknowledgment. Support by NIH Grant 1U54MK074411 is gratefully acknowledged by J.S.L. and I.B. G.M. is grateful

to Ahmet Bakan and Dr. Gunther Stahl from Tripos International for valuable assistance and fruitful discussions.

Supporting Information Available: Pharmacophore model generation, refinement and validation; HPLC purity and NMR data for the tested compounds; expression and purification of recombinant c-Myc-353-437 and Max; screening of c-Myc−Max dimer disruption; competition assay against **1** for c-Myc353-437 binding; electrophoretic mobility shifts assays (EMSA); dose response experiments; cell-based assay. This material is available free of charge via the Internet at http://pubs.acs.org.

References

(1) Nesbit, C. E.; Grove, L. E.; Yin, X.; Prochownik, E. V. Differential apoptotic behaviors of c-Myc, N-Myc, and L-Myc oncoproteins. *Cell Growth Differ.* **1998**, *9*, 731–741.
(2) Soucek, L.; Whitfield, J.; Martins, C. P.; Finch, A. J.; Murphy, D. J.; Sodir, N. M.; Karnezis, A. N.; Swigart, L. B.; Nasi, S.; Evan, G. I. Modelling Myc inhibition as a cancer therapy. *Nature* **2008**, *455*, 679–683.
(3) Amati, B.; Dalton, S.; Brooks, M. W.; Littlewood, T. D.; Evan, G. I.; Land, H. Transcriptional activation by the human c-Myc oncoprotein in yeast requires interaction with Max. *Nature* **1992**, *359*, 423–426.
(4) Amati, B.; Littlewood, T. D.; Evan, G. I.; Land, H. The c-Myc protein induces cell cycle progression and apoptosis through dimerization with Max. *EMBO J.* **1993**, *12*, 5083–5087.
(5) Amati, B.; Brooks, M. W.; Levy, N.; Littlewood, T. D.; Evan, G. I.; Land, H. Oncogenic activity of the c-Myc protein requires dimerization with Max. *Cell* **1993**, *72*, 233–245.
(6) Amati, B. Integrating Myc and TGF-beta signalling in cell-cycle control. *Nat. Cell Biol.* **2001**, *3*, E112–E113.
(7) Wells, J. A.; McClendon, C. L. Reaching for high-hanging fruit in drug discovery at protein−protein interfaces. *Nature* **2007**, *450*, 1001–1009.
(8) Xu, Y.; Lu, H.; Kennedy, J. P.; Yan, X.; McAllister, L. A.; Yamamoto, N.; Moss, J. A.; Boldt, G. E.; Jiang, S.; Janda, K. D. Evaluation of "credit card" libraries for inhibition of HIV-1 gp41 fusogenic core formation. *J. Comb. Chem.* **2006**, *8*, 531–539.
(9) Berg, T.; Cohen, S. B.; Desharnais, J.; Sonderegger, C.; Maslyar, D. J.; Goldberg, J.; Boger, D. L.; Vogt, P. K. Small-molecule antagonists of Myc/Max dimerization inhibit Myc-induced transformation of chicken embryo fibroblasts. *Proc. Natl. Acad. Sci. U.S.A.* **2002**, *99*, 3830–3835.
(10) Kiessling, A.; Sperl, B.; Hollis, A.; Eick, D.; Berg, T. Selective inhibition of c-Myc/Max dimerization and DNA binding by small molecules. *Chem. Biol.* **2006**, *13*, 745–751.
(11) Prochownik, E. V. c-Myc as a therapeutic target in cancer. *Expert Rev. Anticancer Ther.* **2004**, *4*, 289–302.
(12) Wang, H.; Hammoudeh, D. I.; Follis, A. V.; Reese, B. E.; Lazo, J. S.; Metallo, S. J.; Prochownik, E. V. Improved low molecular weight Myc−Max inhibitors. *Mol. Cancer Ther.* **2007**, *6*, 2399–2408.
(13) Yin, X.; Giap, C.; Lazo, J. S.; Prochownik, E. V. Low molecular weight inhibitors of Myc−Max interaction and function. *Oncogene* **2003**, *22*, 6151–6159.
(14) Follis, A. V.; Hammoudeh, D. I.; Wang, H.; Prochownik, E. V.; Metallo, S. J. Binding of small-molecule inhibitors to local sequence sites on the intrinsically disordered c-Myc protein. *Chem Biol.*, in press.
(15) *Pharmacophore Perception, Development, and Use in Drug Design*; International University Line, Biotechnology Series: La Jolla, CA, 2000; pp 1−531.
(16) *Pharmacophores and Pharmacophore Searches*; Wiley-VCH Verlag GmbH & Co. KGaA: Weinheim, Germany, 2008; pp 1−365.
(17) Clark, R. D.; Abrahamian, E. Using a staged multi-objective optimization approach to find selective pharmacophore models. *J. Comput.-Aided Mol. Des.* **2008**, DOI: 10.1007/s10822-008-9227-2.
(18) Richmond, N. J.; Abrams, C. A.; Wolohan, P. R.; Abrahamian, E.; Willett, P.; Clark, R. D. GALAHAD: 1. pharmacophore identification by hypermolecular alignment of ligands in 3D. *J. Comput.-Aided Mol. Des.* **2006**, *20*, 567–587.
(19) Shepphird, J. K.; Clark, R. D. A marriage made in torsional space: using GALAHAD models to drive pharmacophore multiplet searches. *J. Comput.-Aided Mol. Des.* **2006**, *20*, 763–771.
(20) SYBYL 8.0. www.tripos.com.
(21) Irwin, J. J.; Shoichet, B. K. ZINC--a free database of commercially available compounds for virtual screening. *J. Chem. Inf. Model.* **2005**, *45*, 177–182.
(22) Martin, Y. C.; Kofron, J. L.; Traphagen, L. M. Do structurally similar molecules have similar biological activity? *J. Med. Chem.* **2002**, *45*, 4350–4358.
(23) Wallqvist, A.; Huang, R.; Thanki, N.; Covell, D. G. Evaluating chemical structure similarity as an indicator of cellular growth inhibition. *J. Chem Inf. Model.* **2006**, *46*, 430–437.
(24) Covell, D. G.; Huang, R.; Wallqvist, A. Anticancer medicines in development: assessment of bioactivity profiles within the National Cancer Institute anticancer screening data. *Mol. Cancer Ther.* **2007**, *6*, 2261–2269.
(25) ADME Boxes, version 4.0. http://pharma-algorithms.com/.
(26) Japertas, P.; Didziapetris, R.; Petrauskas, A. Fragmental methods in the analysis of biological activities of diverse compound sets. *Mini-Rev. Med. Chem.* **2003**, *3*, 797–808.
(27) Guo, J.; Parise, R. A.; Joseph, E.; Egorin, M. J.; Lazo, J. S.; Prochownik, E. V.; Eiseman, J. L. Efficacy, pharmacokinetics, tisssue distribution, and metabolism of the Myc−Max disruptor, 10058-F4 [*Z*,*E*]-5-[4-ethylbenzylidine]-2-thioxothiazolidin-4-one, in mice. *Cancer Chemother. Pharmacol.* **2008**, *63*, 615–625.
(28) Wrighton, S. A.; Schuetz, E. G.; Thummel, K. E.; Shen, D. D.; Korzekwa, K. R.; Watkins, P. B. The human CYP3A subfamily: practical considerations. *Drug Metab Rev.* **2000**, *32*, 339–361.
(29) ToxBoxes, version 2.0. http://pharma-algorithms.com/.
(30) Schwyzer, R.; Feurer, M.; Iselin, B. Activated esters. III. Reactions of activated esters of amino acid and peptide derivatives with amines and amino acid esters. *Helv. Chim. Acta* **1955**, *38*, 83–91.
(31) Watanabe, S.; Ogawa, K.; Ohno, T.; Yano, S.; Yamada, H.; Shirasaka, T. Synthesis of 4-[1-(substituted phenyl)-2-oxo-pyrrolidin-4-yl]methyloxybenzoic acids and related compounds, and their inhibitory capacities toward fatty-acid and sterol biosynthesis. *Eur. J. Med. Chem.* **1994**, *29* (9), 675–686.
(32) Rothermund, K.; Rogulski, K.; Fernandes, E.; Whiting, A.; Sedivy, J.; Pu, L.; Prochownik, E. V. C-Myc-independent restoration of multiple phenotypes by two C-Myc target genes with overlapping functions. *Cancer Res.* **2005**, *65* (6), 2097–2107.
(33) Uversky, V. N.; Oldfield, C. J.; Dunker, A. K. Intrinsically disordered proteins in human diseases: introducing the D2 concept. *Annu. Rev. Biophys.* **2008**, *37*, 215–246.

JM801278G